Research article

ENST00000534735 inhibits proliferation and migration, promotes apoptosis and pyroptosis of endometrial cancer via OSBPL3 through APMK/SIRT1/NF-κB pathway☆

Shuzhi Shan [a], Xiao Wang [a], Lijie Qian [b], Chunxiao Wang [c], Sufen Zhao [a,*]

[a] *Department of Gynecology and Obstetrics, The Second Hospital of Hebei Medical University, Shijiazhuang, China*
[b] *Hebei Women and Children's Health Center, Shijiazhuang, China*
[c] *Department of Gynecology, Cangzhou People's Hospital, Cangzhou, China*

ABSTRACT

Background: The complete understanding of the biological roles of long non-coding RNAs (lncRNAs) in cancer remains elusive. The findings of this study indicate that the newly discovered lncRNA ENST00000534735 exhibited a decreased expression in both endometrial cancer (EC) tissues and cell lines.
Methods: The expression of ENST00000534735 in EC tissues was detected using RNA-sequencing analysis. The effects of ENST00000534735 on cell proliferation, migration, apoptosis, and pyroptosis were determined via in vitro and in vivo experiments. The proteins that interact with ENST00000534735 were confirmed by RNA pull-down assay. Furthermore, an investigation was conducted on the impact of ENST00000534735 on the in vivo growth of EC through a tumorigenicity assay in nude mice.
Results: We found that ENST00000534735 was significantly down-regulated in EC tissues compared to their adjacent non-cancerous tissues. The ectopic expression of ENST00000534735 drastically inhibited lung cancer cell proliferation and migration ability and facilitated apoptosis and pyroptosis. Knockdown of ENST00000534735 increased OSBPL3 expression, and the tumor-suppressing effects of ENST00000534735 overexpression were reversed by upregulation of OSBPL3 via the APMK/SIRT1/NF-κB pathway. The in vivo tumorigenic assays conducted on nude mice revealed that the excessive expression of ENST00000534735 impeded the growth of EC.
Conclusions: All results elucidated the role and molecular mechanism of ENST00000534735 in the malignant development of EC. ENST00000534735, a new antioncogene in EC, may serve as a survival biomarker or therapeutic target for EC.

1. Introduction

Endometrial cancer (EC) is a common malignant tumor of the female reproductive system, which occurs mainly in perimenopausal and menopausal periods, accounting for 20–30 % of the 3 major malignant tumors in women (second only to ovarian cancer and

cervical cancer) [1,2]. The incidence is highest in Northern Europe and North America, which is 10 times higher than in developing countries. The incidence has recently exhibited an annually increasing trend, which poses a serious threat to women's health [3]. Currently, the clinical treatment methods for EC mainly include surgery, chemotherapy, and radiotherapy, but the treatment effects of the above methods are not ideal for patients with advanced or recurrent EC [4,5]. Therefore, a comprehensive understanding of the molecular mechanism of EC is of great importance for developing its clinical treatment.

Long non-coding RNA (lncRNA) is a class of RNA fragments with a length of more than 200 nucleotides that do not encode proteins. For a long time, it was thought that lncRNA has no biological function [6,7], yet it has now been revealed that lncRNA is a cancer regulator with emerging biological functions and can be used as a biomarker for cancer diagnosis, prognosis, and targeted therapy [8, 9]. For instance, LncRNA SNHG4 modulates EMT Signal and antitumor effects in EC through Transcription Factor SP-1 [10]. LncRNA SLERT promoted promoted EC cell metastasis via regulation of BDNF/TRKB signaling [11]. Nevertheless, with the further research on lncRNAs, there are still numerous newly discovered lncRNAs in the role of EC are not clear.

The study of EC-related lncRNAs is an emerging field of study. Consequently, we attempted to identify novel functional lncRNAs as potential EC targets. We examined 1409 lncRNAs that were substantially differentially expressed between tumor and normal lung tissues. The lncRNA ENST00000534735 was substantially downregulated in EC, as determined by quantitative real-time polymerase chain reaction (qRT-PCR) analysis, and was selected for functional analysis and further study.

2. Methods

2.1. Tissues samples

EC samples and adjacent endometrial tissues were obtained from 23 EC patients undergoing surgical resection from 2018 to 2021 at The Second Hospital of Hebei Medical University (Shijiazhuang, China). During the operation, cancer tissues and adjacent tissues (>4 cm from the edge of the cancer tissue) were taken and placed in liquid nitrogen for later use. The inclusion criteria were as follows: EC confirmed by histopathology; complete clinical data and follow-up records; no history of preoperative radiotherapy and chemotherapy; no hormone therapy in the past 3 months; Patients and their families were aware of the study. The exclusion criteria were as follows: Severe hypertension and diabetes combined with autoimmune disorders (lupus erythematosus, rheumatoid arthritis, etc.); patients simultaneously presenting with other malignant tumors. The Research Ethics Committee of the second hospital of Hebei Medical University approved the protocol (2023-R483).

2.2. RNA-sequencing

The purified total RNA was subjected to ribosomal RNA (rRNA) removal, fragmentation, first-strand complementary DNA (cDNA) synthesis, second-strand cDNA synthesis, end repair, adding A to the 3′-end, ligating, and enriching steps according to the experimental instructions to complete the construction of sequencing sample library. Qubit® 2.0 Fluorometer (Thermo Fisher, Waltham, MA, USA) was used to measure fluorometer concentration, and Agilent 4200 (Agilent, Santa Clara, CA, USA) was used to measure library size. Illumina NovaSeq6000 (Illumina, Santa Clara, CA, USA) sequencing instrument was used for sequencing in PE150 mode.

2.3. Cell culture

EC cell lines (HEC-1B, HEC-1A, KLE, and Ishikawa) and normal endometrial stromal cells (T-HESC) were purchased from the Shanghai Cell Center, Chinese Academy of Sciences (Shanghai, China). EC cell lines were authenticated using (Short Tandem Repeat) STR profiling (Supplementary Fig. 1). The above cells were cultured in Roswell Park Memorial Institute (RPMI) 1640 medium, except the HEC-1A cells were cultured in McCoy's 5A medium, and Ishikawa cells were cultured in Eagle's medium, with 10 % fetal bovine serum (FBS), 100 U/mL of penicillin, and 100 mg/mL of streptomycin. All cells were cultured in a cell culture incubator with 5 % CO_2 and 37 °C saturated humidity.

2.4. Scratch wound healing assay

After 48 h of culture, the cells of each group were seeded into 6-well plates, and the cell density was adjusted to 2×10^5 cells/mL. When the cell confluence degree reached 80 %, the lines were marked on the cell culture surface with a sterile gun tip. Images were taken under an inverted microscope at 0 and 24 h, and the distance between cell scratches was measured and analyzed by Image J software (National Institutes of Health, Bethesda, MD, USA). Scratch healing rate = (0 h scratch spacing − 48 h scratch spacing)/0 h scratch spacing × 100.00 %.

2.5. Cell transfection

pcDNA3. 1-ENST00000534735 and its negative control pcDNA3.1, si-ENST00000534735 (Forward, 5′-CGCUGGUGUGUGCCUU-GUAGU-3'; Reverse, 5′-UACAAGGCACACACCAGCGUG-3′), and its negative control si-vector, and si-OSBPL3 (Forward, 5′-GUU-GAAUUGUGUUAUCAAAGC-3'; Reverse, 5′-UUUGAUAACACAAUUCAACUA-3′), and negative control si-NC were obtained from Shanghai GenePharma (Shanghai, China). The cells were seeded in 6-well plates at 1×10^5 cells per well for cell transfection. When the confluence of the cells reached 70 % density, the cells, after transfection for 48 h, were collected for subsequent experiments in strict

accordance with the instructions of the Lipofectamine 3000 reagent (Thermo Fisher).

2.6. Proliferation assay

The transfected cells of each group were seeded in a 96-well plate at a density of 5×10^3 cells/well, and after 48 h, 10 μL Cell Counting Kit-8 (CCK-8) was added (Beyotime Biotechnology, Shanghai, China). After 2 h, the cell absorbance at 450 nm was measured by a microplate reader.

2.7. Cell apoptosis assay

An Annexin V-FITC Apoptosis Detection Kit (Beyotime) was used to detect the apoptosis of cells. Cells from each group were resuspended in 500 μL of $1 \times$ binding buffer and subsequently incubated with 5 μL Annexin V-FITC and 5 μL propidium iodide (PI) in the dark at room temperature for 10 min. Finally, samples were analyzed for apoptosis by flow cytometry.

2.8. RNA immunoprecipitation assay

The RNA-Binding Protein Immunoprecipitation kit (Millipore, Burlington, MA, USA) was utilized to accomplish the RNA immunoprecipitation (RIP) assay. Cells were lysed in lysis buffer, and the cell lysates were incubated with magnetic beads conjugated to human anti-argonaute2 (Ago2) antibody or anti-IgG. The enrichment of ENST00000534735 and OSBPL3 was tested using qRT-PCR.

2.9. Nude mouse tumorigenicity assay

A total of 20 female BALB/c nude mice (aged 4–6 weeks old and weighing 18–20 g) were acquired from the Vital River Laboratory Animal Center (Beijing, China). The nude mice were randomly allocated to 4 groups (si-NC, si-ENST00000534735, pcDNA3.1, pcDNA3.1-ENST00000534735) of 5 mice based on their body weight and reared in a specific-pathogen-free (SPF) environment. 2×10^6 cells were implanted subcutaneously into nude mice to form tumors. When the maximum diameter of tumors reached about 1 cm, the nude mice underwent uniform euthanasia, and the tumor tissues were stripped, photographed, and weighed. After paraffin embedding and sectioning, interleukin (IL)-18 (1:100; Proteintech, Rosemont, IL, USA) and IL-1β (1:500, Proteintech) primary antibodies and horseradish peroxidase (HRP)-labeled secondary antibodies (1:2,000, Abcam, Cambridge, UK) were incubated. The expression levels of IL-18 and IL-1β protein in tissue samples were detected. For the histopathological examination, sections were stained with hematoxylin and eosin (HE). The TdT-mediated biotinylated nick end-labeling (TUNEL) staining procedure followed the manufacturer's instructions before using a light microscope analysis. The Ethics Committee of The Second Hospital of Hebei Medical University approved the study (No. 2022-AE298).

2.10. qRT-PCR

Total RNA of the tissues or cells were extracted using the total RNA extraction kit (Invitrogen, Carlsbad, CA, USA), reverse transcribed into complementary DNA, and polymerase chain reaction (PCR) was performed according to the primer sequence. The PCR reaction conditions were as follows: predenaturation at 94 °C for 2 min; 40 cycles of denaturation at 94 °C for 20 s, annealing at 58 °C for 45 s, and extension at 72 °C for 45 s were repeated, followed by extension at 72 °C for 5 min. The $2^{-\Delta\Delta Ct}$ technique was used to quantify the quantitative expression of target genes. The primer sequences were as follows: ENST00000534735 (forward primer: 5′-TTGATCACGTTGGGGAGAACAG-3′; reverse primer: 5′-GACAAGGATGGCTGCTCCTG-3′) and β-actin (forward primer: 5′-CTTCGCGGGCGACGAT-3″; reverse primer: 5′-CCACATAGGAATCCTTCTGACC-3′).

2.11. Western blot assay

The protein expression of cleaved-Caspase-3, GSDME-N, NLRP3, and OSBPL3 and the levels of *p*-AMPK/AMPK, SIRT1, and NF-κB were detected in each group. The total protein content of tissues and cells was extracted by following the instructions provided by the protein extraction kit. The bicinchoninic acid (BCA) method detected the protein concentration and the final concentration was adjusted to 5 μg/μL. Then, 4 μL of the tested sample was subjected to electrophoresis, transferred to the membrane, and blocked. The primary antibody was added (dilution ratio 1:1000), incubated at 4 °C overnight, and washed. HRP-labeled secondary antibody (dilution ratio 1:5000) was added and incubated at room temperature for 2 h. The color reaction was performed, and the gray value of the target protein was analyzed. Primary antibody contained cleaved caspase-3 antibody (#9661; Cell Signaling Technology), GSDME-N antibody (ab21591; Abcam), NLRP3 antibody (ab263899; Abcam), OSBPL3 antibody (orb412299; biorbyt), Anti-*p*-AMPK antibody (ab131357; Abcam), Anti-AMPK antibody (ab32047; Abcam), SIRT1 antibody (ab189494; Abcam), NF-κB antibody (ab16502; Abcam), and β-actin antibody (ab8226; Abcam).

2.12. Statistical analysis

The mean ± standard error means (SEM) was used to express the data. ANOVA was used to compare three or more experimental groups, whereas the student's *t*-test compared two groups. Significance was defined as $*p < 0.05$, $**p < 0.01$, $***p < 0.001$. All
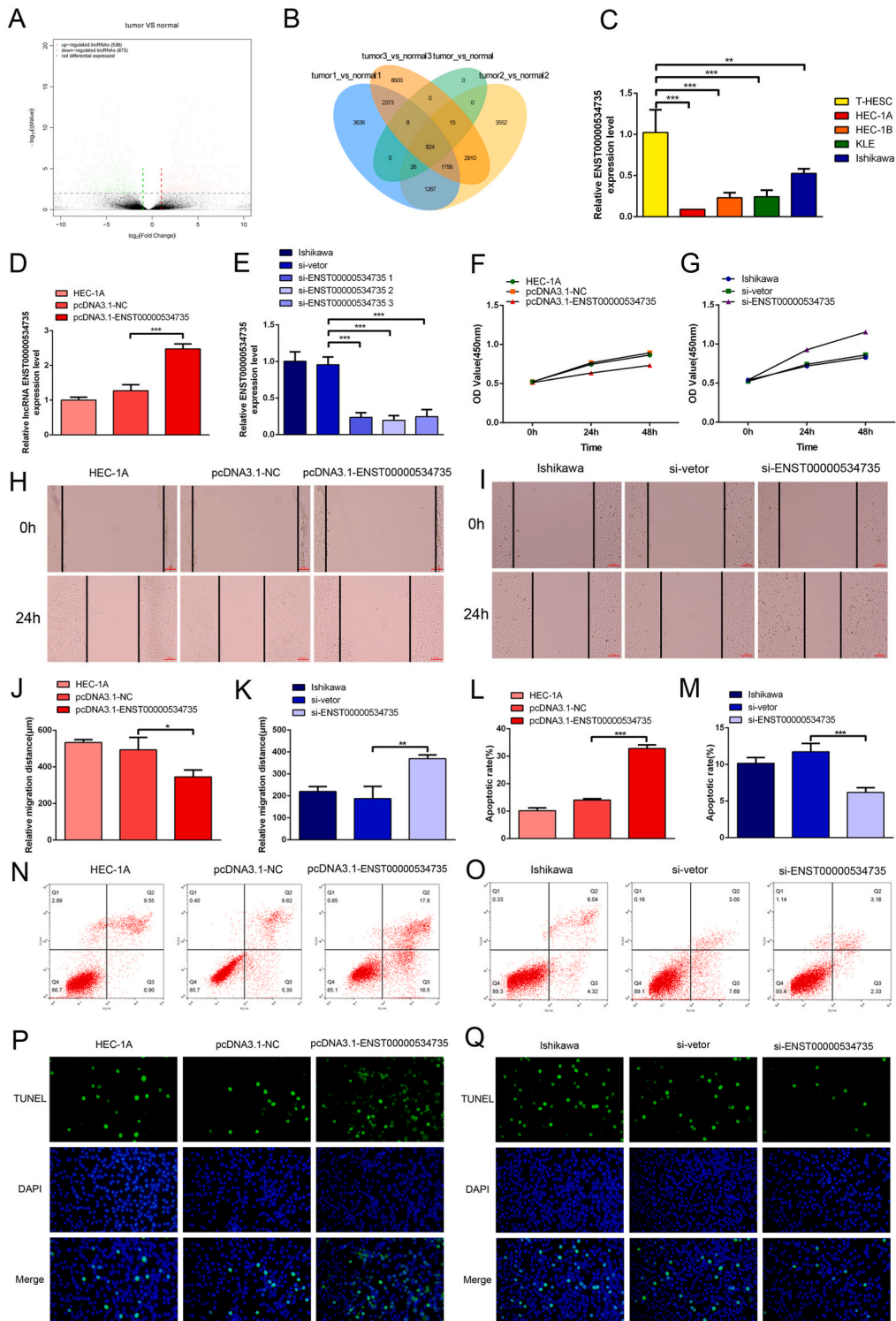
Fig. 1. ENST00000534735 overexpression inhibits cell growth and migration and promotes apoptosis of EC cells. (A) Volcano plots of the differentially expressed lncRNAs in EC tissues and adjacent normal tissues generated from RNA-seq; (B) Venn diagram showing the overlap between EC tissues and adjacent normal tissues; (C) the expression levels of ENST00000534735 in EC cell lines by RT-PCR; (D) ENST00000534735 expression in HEC-1A cells with pcDNA3.1-ENST00000534735 or pcDNA3.1-NC; (E) NST00000534735 expression in Ishikawa cells with si-ENST00000534735 or si-vector; (F) pcDNA3.1-ENST00000534735 inhibited cell proliferation in HEC-1A cells; (G) pcDNA3.1-ENST00000534735 increased cell proliferation in Ishikawa cells; (H–K) the migration of EC cells was measured using a wound healing assay and the corresponding quantitative results; (L–O) the apoptosis of EC cells was measured using a flow cytometry assay and the corresponding quantitative results; (P,Q)

apoptotic cells were assessed by TUNEL (magnification, × 200). Data are expressed as mean ± SEM. *, P < 0.05; **, P < 0.01; ***, P < 0.001. EC, endometrial cancer; lncRNA, long non-coding RNA; RT-PCR, real-time polymerase chain reaction; TUNEL, TdT-mediated biotinylated nick end-labeling; SEM, standard error means.

statistical analyses were performed using GraphPad Prism 8.0.

3. Results

3.1. ENST00000534735 overexpression inhibits cell growth and migration and promotes the apoptosis of EC cells

According to the results of the RNA sequencing, a total of 1409 lncRNAs were identified (873 downregulated genes and 536 upregulated genes), the most downregulated lncRNA in tumor tissues compared with normal tissue caught our attention among most of the uncharacterized lncRNAs (Fig. 1A and B). Further, ENST00000534735 expression was decreased in EC cells (HEC-1B, HEC-1A, KLE, and Ishikawa) than in T-HESC cells (Fig. 1C). To investigate the function and role of ENST00000534735 in EC, si-ENST00000534735, and si-vector groups were transfected into Ishikawa cells, and pcDNA3.1-ENST00000534735 and its negative control pcDNA3.1-NC groups were transfected into HEC-1A. ENST00000534735 expression was higher when treated with ENST00000534735 overexpression (Fig. 1D) and lower when treated with si-ENST00000534735 (Fig. 1E). The CCK-8 assay showed that overexpression of ENST00000534735 significantly inhibited the proliferation ability of EC cells compared with the pcDNA3.1-NC group (Fig. 1F), whereas downregulation of ENST00000534735 may have increased cell proliferation (Fig. 1G). Furthermore, wound healing analysis validated that the migratory ability of human HEC-1A and Ishikawa cells was markedly reduced when ENST00000534735 was overexpressed (Fig. 1H–K). The data from flow cytometry (Fig. 1L–O) and TUNEL assay (Fig. 1P–Q) analysis revealed that ENST00000534735 overexpression markedly induced cell apoptosis, whereas downregulation of ENST00000534735 may decrease cell apoptosis.

3.2. ENST00000534735 regulates EC pyroptosis

To understand the mechanism of the antitumor effect of ENST00000534735, protein levels of IL-1β and IL-18 were detected after transfection with pcDNA3.1-ENST00000534735 or si-ENST00000534735. As shown in Fig. 2A–D, overexpression of ENST00000534735 significantly increased IL-1β and IL-18 levels, and knockdown by si-ENST0000053473 inhibited IL-1β and IL-18 levels. Further, overexpression of ENST00000534735 significantly increased cleaved caspase 1, GSDME-N, and NLRP3 levels, and knockdown of ENST00000534735 suppressed expressions of cleaved caspase 1, GSDME-N, and NLRP3 as detected by Western blot (WB) (Fig. 2E).
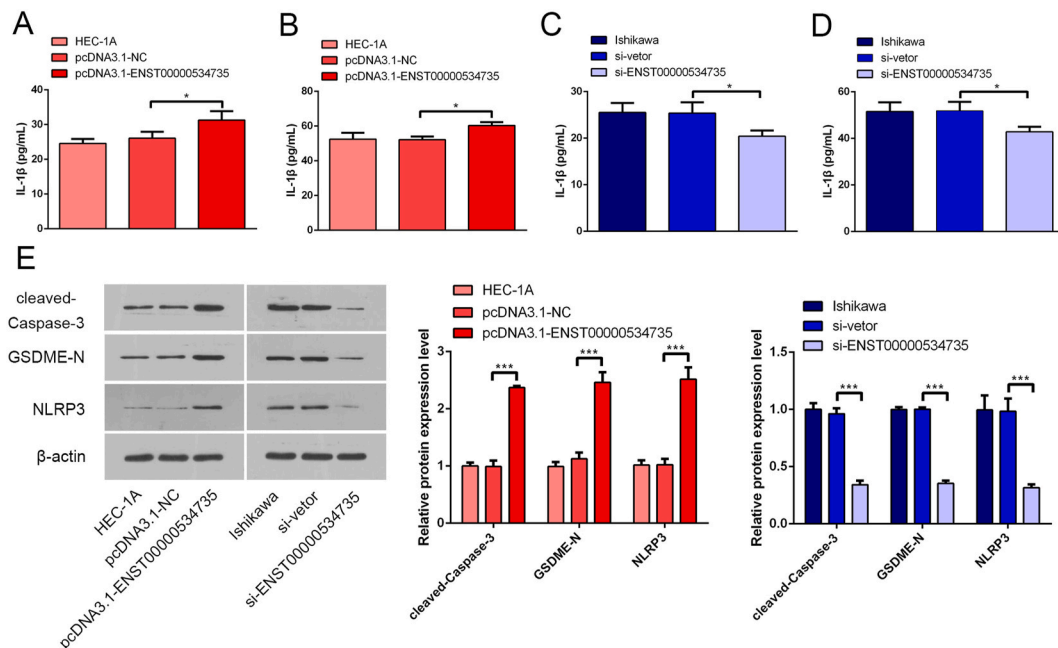
Fig. 2. ENST00000534735 regulates EC pyroptosis. (A–D) ELISA measured the levels of IL-1β and IL-18 in HEC-1A and Ishikawa cells; (E) the expressions of cleaved caspase 1, GSDME-N, and NLRP3 were detected by WB. Uncropped WB images are shown in Supplementary Fig. 2. Results are presented as mean ± SEM; *, P < 0.05; ***, P < 0.001. EC, endometrial cancer; ELISA, enzyme-linked immunosorbent assay; WB, Western blot.
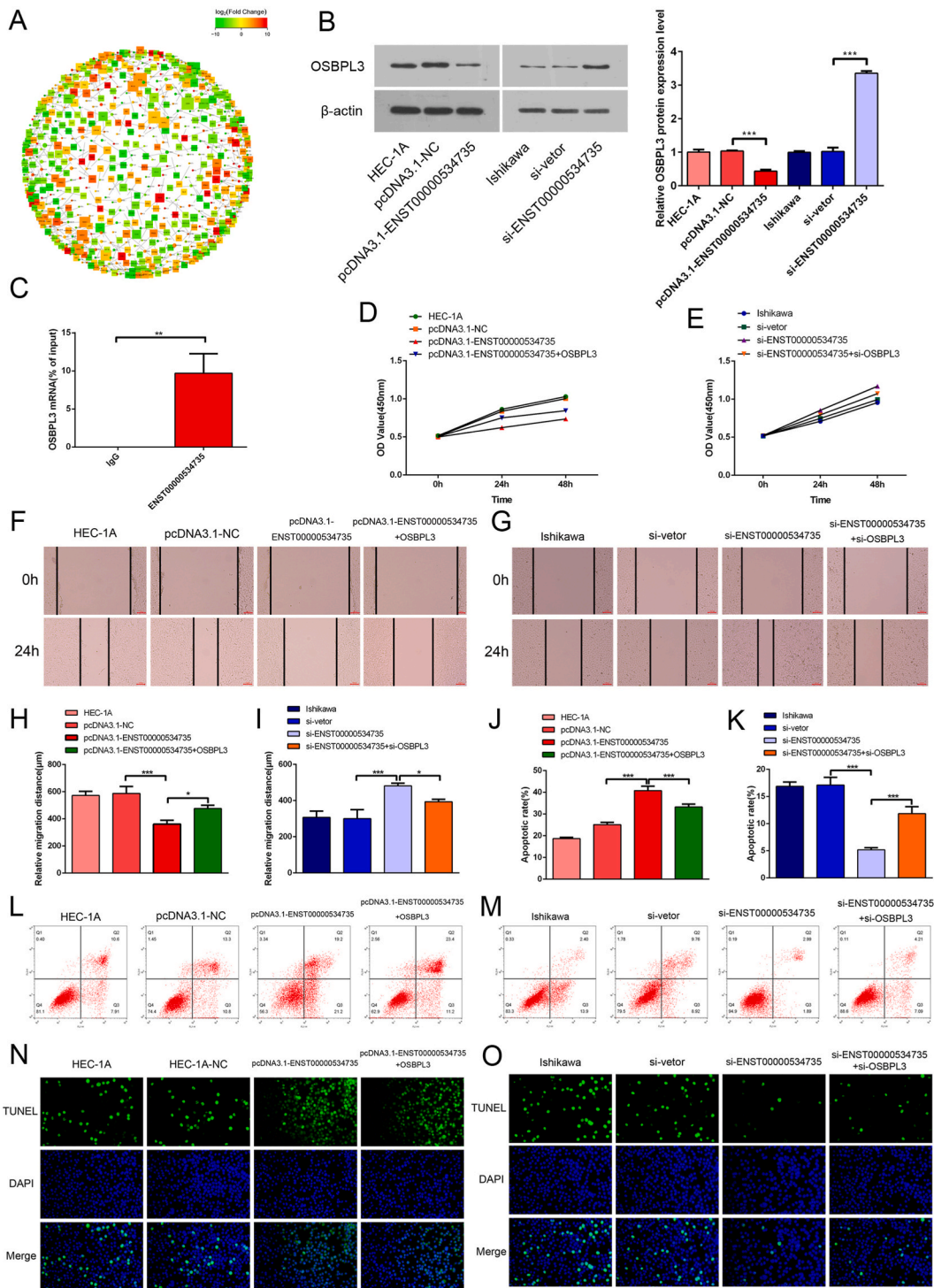
Fig. 3. OSBPL3 interacted with ENST00000534735. (A) LncRNA-mRNA correlation network; (B) the protein expression of OSBPL3 was measured using WB and uncropped WB images are shown in Supplementary Fig. 3; (C) the interplay between ENST00000534735 and OSBPL3 was detected by RIP assay; (D, E) CCK-8 assay tested the proliferation of HEC-1A and Ishikawa cells; (F–I) the migration of EC cells was measured using a wound healing assay and the corresponding quantitative results; (J–M) the apoptosis of EC cells was measured using a flow cytometry assay and the corresponding quantitative results; (N, O) the apoptosis of EC cells was stained by TUNEL (magnification, × 200). Results are presented as mean ± SEM. *, P < 0.05; **, P < 0.01; ***, P < 0.001. lncRNA, long non-coding RNA; mRNA, messenger RNA; EC, endometrial cancer; RIP, RNA immunoprecipitation.

3.3. ENST00000534735 regulate EC cells growth, migration, and apoptosis through OSBPL3

Previous studies have verified that lncRNAs could exhibit *cis*-regulatory properties with their nearby coding genes. The downstream proteins of ENST00000534735 were screened in the sequencing results, and OSBPL3 was shown to be a downstream protein of ENST00000534735 and was significantly overexpressed in the sequencing results (Fig. 3A). The expression of OSBPL3 protein was decreased in the pcDNA3.1-ENST00000534735 group and increased in the si-ENST00000534735 group (Fig. 3B). In addition, as shown in Fig. 3C, ENST00000534735 could directly bind to OSBPL3, which was verified by the RIP assay. To confirm the molecular mechanism of ENST00000534735 and OSBPL3 in EC, OSBPL3 overexpressed plasmid or si-OSBPL3 was transfected into EC cells. The results of the CCK-8, scratch wound healing, flow cytometry, and TUNEL assays showed that the overexpression of OSBPL3 could reverse the effect of pcDNA3.1-ENST00000534735 for proliferation, migration, and apoptosis in HEC-1A cells. In contrast, inhibition of OSBPL3 could reverse the effect of si-ENST00000534735 for proliferation, migration, and apoptosis in Ishikawa cells (Fig. 3D–O).

### 3.4. ENST00000534735 regulates EC cell pyroptosis through OSBPL3

To investigate whether ENST00000534735 regulates pyroptosis through OSBPL3, OSBPL3 was overexpressed or inhibited in EC cells. The results showed that overexpression of OSBPL3 could reverse the increased levels of IL-1β and IL-18 in the supernatant, while the downregulation of OSBPL3 decreased their expression caused by overexpression of ENST00000534735 (Fig. 4A–D). Moreover, overexpression or downregulation of OSBPL3 could partially reverse the increase or reduce cleaved caspase 1, GSDME-N, and NLRP3 protein levels due to ENST00000534735 upregulation or downregulation. (Fig. 4E).

3.5. ENST00000534735/OSBPL3 inhibits EC cell function through the inactivation of the APMK/SIRT1/NF-κB pathway

In the WB experiment (Fig. 5A), the phosphorylation levels of APMK, SIRT1, and NF-κB in the pcDNA3.1-ENST00000534735 group were significantly increased, and the levels of these proteins were significantly decreased after overexpression of OSBPL3. To investigate whether ENST00000534735/OSBPL3 regulates EC cell metastasis through the APMK/SIRT1/NF-κB pathway, the AMPK activator, AICAR, was used to activate AMPK signaling. As shown in Fig. 5B, the pcDNA3.1-ENST00000534735 + OSBPL3 + activator group increased the expression levels of the *p*-APMK, SIRT1, and NF-κB compared with the pcDNA3.1-ENST00000534735 + OSBPL3 group. Moreover, si-ENST00000534735 + si-OSBPL3 + activator groups increased the expression levels of the *p*-APMK, SIRT1, and NF-κB compared with the si-ENST00000534735 + si-OSBPL3 group. In addition, the CCK-8 and TUNEL assays show that the AMPK activator therapy considerably reversed the effect of pcDNA3.1-ENST00000534735 + OSBPL3 or si-ENST00000534735 + si-OSBPL3 for proliferation and apoptosis in HEC-1A and Ishikawa cell, suggesting that the APMK/SIRT1/NF-κB pathway was an essential mechanism mediating the function of ENST00000534735 and OSBPL3 in EC (Fig. 5C–F).
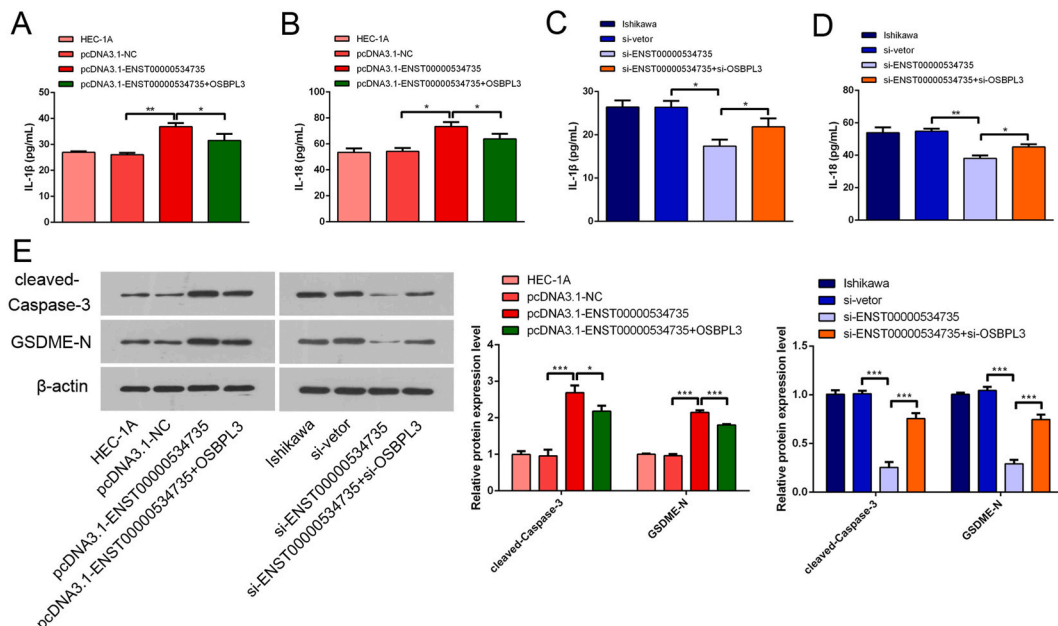

Fig. 4. ENST00000534735 regulates EC cell pyroptosis through OSBPL3. (A–D) ELISA measured the levels of IL-1β and IL-18 in HEC-1A and Ishikawa cells was used to detect the expression of pyroptosis markers IL-18 and IL-1β; (E) the expressions of cleaved caspase 1, GSDME-N, and NLRP3 were detected by WB. Uncropped WB images are shown in Supplementary Fig. 4. Results are presented as mean ± SEM. *, P < 0.05; **, P < 0.01; ***, P < 0.001. EC, endometrial cancer; ELISA, enzyme-linked immunosorbent assay; WB, Western blot.
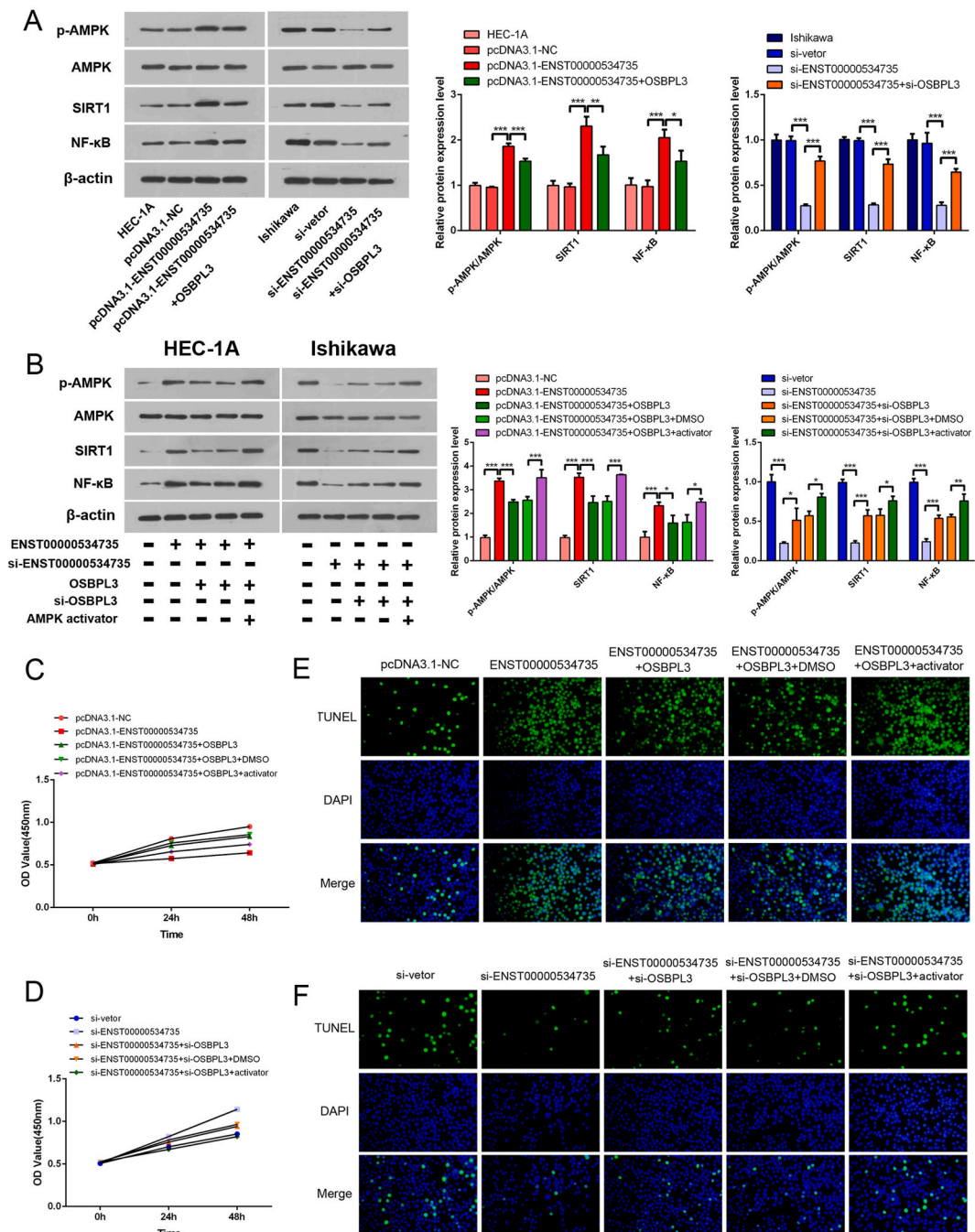
Fig. 5. ENST00000534735/OSBPL3 regulates cell growth apoptosis through the APMK/SIRT1/NF-κB pathway. (A, B) Relative expression levels of *p*-APMK, APMK, SIRT1, and NF-κB and their density quantification results. Uncropped WB images are shown in Supplementary Figs. 5 and 6; (C, D) CCK-8 analysis of the viability; (E, F) the changes in the apoptotic ability of the cells was detected by TUNEL (magnification, × 200). CCK-8, cell counting kit-8; TUNEL, TdT-mediated biotinylated nick end-labeling.

Enzyme-linked immunosorbent assay (ELISA) and WB further detected pyroptosis-related proteins. As shown in Fig. 6A–D, the results showed that AMPK activator therapy considerably reversed the levels of IL-1β and IL-18 in the supernatant by overexpression or downregulation of ENST00000534735 and OSBPL3. More importantly, the relative levels of cleaved caspase 1, GSDME-N, and NLRP3 in the pcDNA3.1-ENST00000534735 + OSBPL3 + activator group were much higher than those in the pcDNA3.1-ENST00000534735 + OSBPL3 group (Fig. 6E).
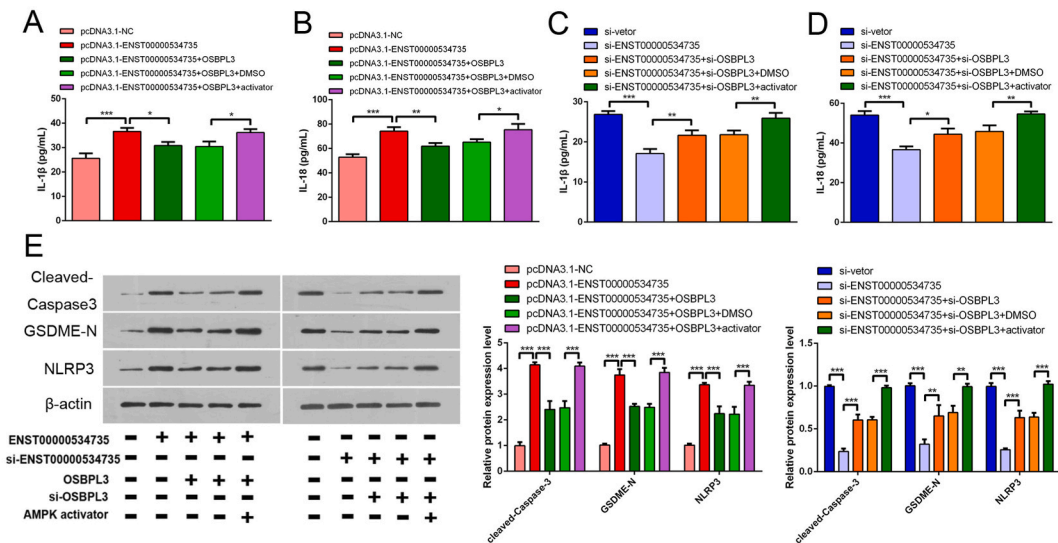
Fig. 6. ENST00000534735/OSBPL3 regulates cell growth apoptosis through the APMK/SIRT1/NF-κB pathway. (A–D) ELISA was used to detect the expression of pyroptosis markers IL-18 and IL-1β; (E) WB was used to detect the expression of pyroptosis-related proteins cleaved-Caspase-3, GSDME-N, and NLRP3. Uncropped WB images are shown in Supplementary Fig. 7. ELISA, enzyme-linked immunosorbent assay; WB, Western blot.

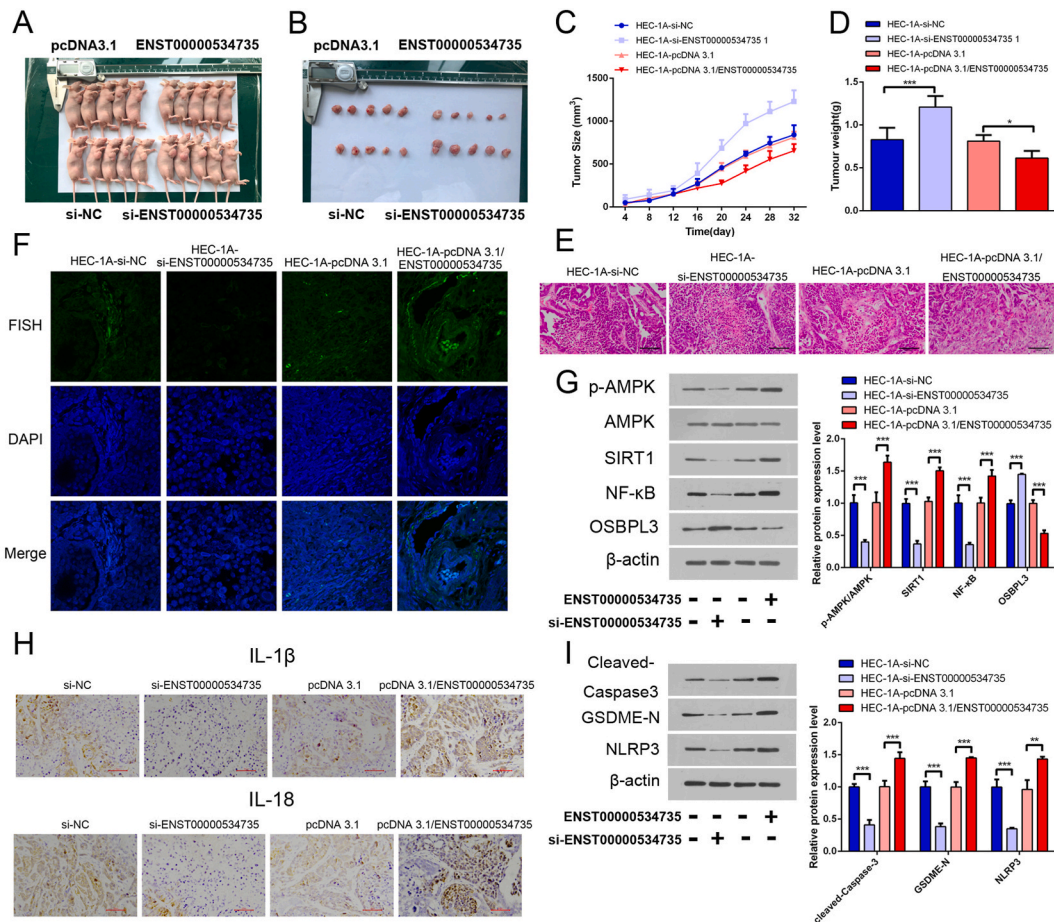### 3.6. ENST00000534735 regulates tumor growth in vivo

To further confirm that ENST00000534735 affected tumor growth in vivo, HEC-1A cells were transfected with si-ENST00000534735 or pcDNA3.1-ENST00000534735 injected into nude mice. Over the 32 days following injection, the tumor size and weight with low expression of ENST00000534735 were increased, whereas those of the tumors with high expression of ENST00000534735 were decreased (Fig. 7A–D). The xenograft tumor tissues were confirmed by HE staining (Fig. 7E), and the expression of ENST00000534735 in the sections of the excision tumor was detected. The ENST00000534735 level was decreased in the HEC-1A-si-ENST00000534735 group and increased in the HEC-1A-pcDNA3.1-ENST00000534735 group (Fig. 7F). WB confirmed that ENST00000534735 knockdown could inhibit *p*-APMK, SIRT1, and NF-κB and promote OSBPL3 level, whereas overexpression of ENST00000534735 promoted *p*-APMK, SIRT1, and NF-κB and inhibited OSBPL3 level (Fig. 7G). Immunohistochemistry (IHC) showed that silencing ENST00000534735 inhibited tumor IL-1β and IL-18 expression, whereas overexpression of ENST00000534735 promoted tumor IL-1β and IL-18 expression (Fig. 7H). In addition, as shown in Fig. 7I, the relative levels of cleaved caspase 1, GSDME-N, and NLRP3 were decreased in the HEC-1A-si-ENST00000534735 group, whereas they were increased in the HEC-1A-pcDNA3.1-ENST00000534735 group.

4. Discussion

High-throughput RNA sequencing and bioinformatics have accelerated our understanding of lncRNAs, a subset of ncRNAs with a length >200 nucleotides that may function as oncogenes or tumor suppressor genes and exert diverse biological effects on cancers such as EC [12,13]. Growing evidence suggests that lncRNAs play an important role in carcinogenesis by controlling several cellular processes, including cell division, migration, invasion, apoptosis, pyroptosis, and metastasis [14,15]. According to research published by Du et al. [16], lncRNA DLEU1 accelerated the growth of EC by binding to mTOR, which led to an upregulation of the PI3K/AKT/mTOR pathway. Fang et al. discovered that the lncRNA ENST00000585827 controlled the miR-424/E2F6/E2F7 signaling axis and to suppress the uncontrolled growth of EC cells [17].

The current investigation revealed that the levels of expression of the recently discovered ENST00000534735 were diminished in both EC tissues and cell lines. This suggests that ENST00000534735 may play a crucial role in developing EC tumors. The biological function of ENST00000534735 was subsequently assessed in EC cells, and the associated molecular mechanisms were investigated. The findings indicate that the expression of ENST00000534735 inhibited the growth and movement of EC cells while inducing programmed and inflammatory cell death.

Although lncRNAs do not encode functional proteins, they exert biological functions through influencing other protein coding genes [18]. Our study identified OSBPL3, a differentially expressed gene positively correlated with ENST0000053473 expression. OSBPL3 is a member of the OSBP family, which comprises 12 members, namely OSBP, OSBPL1-OSBPL11. The OSBP gene sequences are a closely related family that exhibit two primary structures, namely a highly conserved oxysterol domain located at the C-terminal and, in most instances, a pleckstrin homology (PH) domain situated at the N-terminal [19,20]. There is speculation that OSBP is involved in various cellular processes, such as lipid metabolism, vesicle transport, and cell signaling, as indicated by previous research [21]. In contrast to early breast cancer, OSBPL3 exhibited a higher frequency of mutations in metastatic breast cancer, which was

Fig. 7. ENST00000534735 regulates tumor growth in vivo. (A, B) Female nude mice were intrasplenically transplanted with HEC-1A cells, randomized, and divided into 4 groups (n = 6/group). 32 days after implantation, mice were sacrificed. Tumors were harvested; (C, D) tumor size and weight of mice; (E) Xenograft tumor tissues were confirmed by HE staining; (F) FISH assay displayed the location of ENST00000534735 (green) in tumor tissue (magnification, × 200); (G) the expression of OSBPL3, p-AMPK/AMPK, SIRT1, and NF-κB in tumor tissues was detected by WB. Uncropped WB images are shown in Supplementary Fig. 8; (H) IHC detected the expression of IL-18 and IL-1β in tumor tissues (magnification, × 200); (I) WB was used to detect the expression of pyroptosis-related proteins cleaved-Caspase-3, GSDME-N, and NLRP3. Uncropped WB images are shown in Supplementary Fig. 9. FISH, fluorescence in-situ hybridization; HE, hematoxylin and eosin; WB, Western blot; IHC, immunohistochemistry. (For interpretation of the references to color in this figure legend, the reader is referred to the Web version of this article.)

correlated with unfavorable outcomes [22]. Additionally, Njeru et al. proposed that OSBPL3 mutations may play a role in carcinogenesis by disrupting multiple molecular processes, including lipid metabolism, proliferation, and cell survival [23]. A recent study found that OSBPL3 is a novel driver gene stimulating the R-Ras/Akt signaling pathway and a potential therapeutic target in gastric cancer patients [24]. These biological functions of OSBPL3 have been revealed after the completion of this study, which further supports the present evidence. Considering the defined role of AMPK in tumorigenesis [25], our research aimed to elucidate the potential biological effects of ENST00000534735 on EC. Knockdown of SIRT1 promotes pyroptosis [26] and inhibits tumor proliferation [27]. Studies have shown that metformin activates the AMPK/SIRT1/NF-κB pathway to drive caspase3/GSDME-mediated pyroptosis in cancer cells [28]. Our study found ENST00000534735/OSBPL3 inhibits EC cell function by inactivating the APMK/SIRT1/NF-κB pathway. These findings indicated that the tumor-suppressing effects of ENST00000534735 on EC cells are partially mediated through the OSBPL3 via APMK/SIRT1/NF-κB pathway. The present study has limitations, including a restricted number of patients. Moreover, the mechanisms ENST00000534735 participates in EC progression remain to be elucidated.

In conclusion, our study found a new antioncogene in EC, LncRNA ENST00000534735, inhibits proliferation and migration and promotes apoptosis and pyroptosis of EC via OSBPL3 through the APMK/SIRT1/NF-κB pathway. These findings provide new insights into the clinical diagnosis and prognosis of EC.

Funding

Ethics statement

The studies involving animal experiments (2022-AE298) and human participants (2023-R483) were reviewed and approved by Ethics Committee of the Second Hospital of Hebei Medical University.

Data availability

Data will be made available on request.

CRediT authorship contribution statement

Shuzhi Shan: Writing – original draft, Formal analysis, Data curation. **Xiao Wang:** Writing – review & editing, Methodology, Formal analysis. **Lijie Qian:** Writing – review & editing, Data curation. **Chunxiao Wang:** Writing – review & editing, Data curation. **Sufen Zhao:** Writing – review & editing, Supervision, Project administration.

Declaration of competing interest

The authors declare that they have no known competing financial interests or personal relationships that could have appeared to influence the work reported in this paper.

Appendix A. Supplementary data

Supplementary data to this article can be found online at https://doi.org/10.1016/j.heliyon.2024.e25281.

References

[1] L. Vermij, V. Smit, R. Nout, T. Bosse, Incorporation of molecular characteristics into endometrial cancer management, Histopathology 76 (1) (2020) 52–63, https://doi.org/10.1111/his.14015.

[2] M. Gjorgoska, T. Rizner, Integration of androgen hormones in endometrial cancer biology, Trends in endocrinology and metabolism: TEM (Trends Endocrinol. Metab.) 33 (9) (2022) 639–651, https://doi.org/10.1016/j.tem.2022.06.001.

[3] Y. Aoki, H. Kanao, X. Wang, M. Yunokawa, K. Omatsu, A. Fusegi, et al., Adjuvant treatment of endometrial cancer today, Jpn. J. Clin. Oncol. 50 (7) (2020) 753–765, https://doi.org/10.1093/jjco/hyaa071.

[4] B. Gu, X. Shang, M. Yan, X. Li, W. Wang, Q. Wang, et al., Variations in incidence and mortality rates of endometrial cancer at the global, regional, and national levels, 1990-2019, Gynecologic oncology 161 (2) (2021) 573–580, https://doi.org/10.1016/j.ygyno.2021.01.036.

[5] E.J. Crosbie, S.J. Kitson, J.N. McAlpine, A. Mukhopadhyay, M.E. Powell, N. Singh, Endometrial cancer, Lancet (London, England) 399 (10333) (2022) 1412–1428, https://doi.org/10.1016/s0140-6736(22)00323-3.

[6] H. Liu, J. Wan, J. Chu, Long non-coding RNAs and endometrial cancer, Biomedicine & pharmacotherapy = Biomedecine & pharmacotherapie 119 (2019) 109396, https://doi.org/10.1016/j.biopha.2019.109396.

[7] C. Vallone, G. Rigon, C. Gulia, A. Baffa, R. Votino, G. Morosetti, et al., Non-Coding RNAs and Endometrial Cancer 9 (4) (2018), https://doi.org/10.3390/genes9040187.

[8] F. Aljubran, W.B. Nothnick, Long non-coding RNAs in endometrial physiology and pathophysiology, Mol. Cell. Endocrinol. 525 (2021) 111190, https://doi.org/10.1016/j.mce.2021.111190.

[9] W. He, Y. Chen, L. Wu, Y. Guo, Z. You, G. Yang, A novel necroptosis-related lncRNA signature for predicting prognosis and anti-cancer treatment response in endometrial cancer, Front. Immunol. 13 (2022) 1018544, https://doi.org/10.3389/fimmu.2022.1018544.

[10] L.K. Kim, S.A. Park, LncRNA SNHG4 modulates EMT signal and antitumor effects in endometrial cancer through Transcription Factor SP-1 11 (4) (2023), https://doi.org/10.3390/biomedicines11041018.

[11] J. Tian, H. Cheng, N. Wang, C. Wang, SLERT, as a novel biomarker, orchestrates endometrial cancer metastasis via regulation of BDNF/TRKB signaling, World J. Surg. Oncol. 21 (1) (2023) 27, https://doi.org/10.1186/s12957-022-02821-w.

[12] J. Sun, L. Li, H. Chen, L. Gan, X. Guo, J. Sun, Identification and validation of an m7G-related lncRNAs signature for prognostic Prediction and immune function analysis in endometrial cancer, Genes 13 (8) (2022), https://doi.org/10.3390/genes13081301.

[13] J. Bieńkiewicz, H. Romanowicz, B. Szymańska, D. Domańska-Senderowska, M. Wilczyński, A. Stepowicz, et al., Analysis of lncRNA sequences: FAM3D-AS1, LINC01230, LINC01315 and LINC01468 in endometrial cancer, BMC Cancer 22 (1) (2022) 343, https://doi.org/10.1186/s12885-022-09426-2.

[14] W. Lv, Y. Tan, C. Zhao, Y. Wang, M. Wu, Y. Wu, et al., Identification of pyroptosis-related lncRNAs for constructing a prognostic model and their correlation with immune infiltration in breast cancer 25 (22) (2021) 10403–10417, https://doi.org/10.1111/jcmm.16969.

[15] S.J. Liu, H.X. Dang, Long noncoding RNAs in cancer metastasis 21 (7) (2021) 446–460, https://doi.org/10.1038/s41568-021-00353-1.

[16] Y. Du, L. Wang, S. Chen, Y. Liu, Y. Zhao, lncRNA DLEU1 contributes to tumorigenesis and development of endometrial carcinoma by targeting mTOR 57 (9) (2018) 1191–1200, https://doi.org/10.1002/mc.22835.

[17] D. Fang, Q. Zhang, M. Mu, Q. Deng, Y. Wang, Q. Li, lncRNA ENST00000585827 contributes to the progression of endometrial carcinoma via regulating miR-424/E2F6/E2F7 Axis, Appl. Biochem. Biotechnol. 195 (5) (2023) 3096–3108, https://doi.org/10.1007/s12010-022-04267-y.

[18] F. Kopp, J.T. Mendell, Functional classification and experimental dissection of long noncoding RNAs, Cell 172 (3) (2018) 393–407, https://doi.org/10.1016/j.cell.2018.01.011.

[19] N. Hao, Y. Zhou, Y. Li, H. Zhang, B. Wang, X. Liu, et al., Clinical value and potential mechanisms of oxysterol-binding protein like 3 (OSBPL3) in human tumors, Front. Mol. Biosci. 8 (2021) 739978, https://doi.org/10.3389/fmolb.2021.739978.

[20] M. Lehto, M.I. Mäyränpää, T. Pellinen, P. Ihalmo, S. Lehtonen, P.T. Kovanen, et al., The R-Ras interaction partner ORP3 regulates cell adhesion, J. Cell Sci. 121 (Pt 5) (2008) 695–705, https://doi.org/10.1242/jcs.016964.

[21] Y. Zhou, G. Wohlfahrt, J. Paavola, V.M. Olkkonen, A vertebrate model for the study of lipid binding/transfer protein function: conservation of OSBP-related proteins between zebrafish and human, Biochemical and biophysical research communications 446 (3) (2014) 675–680, https://doi.org/10.1016/j.bbrc.2013.12.002.

[22] C. Lefebvre, T. Bachelot, T. Filleron, Mutational profile of metastatic breast cancers, A Retrospective Analysis 13 (12) (2016) e1002201, https://doi.org/10.1371/journal.pmed.1002201.

[23] S.N. Njeru, J. Kraus, J.K. Meena, Aneuploidy-inducing gene knockdowns overlap with cancer mutations and identify Orp3 as a B-cell lymphoma suppressor 39 (7) (2020) 1445–1465, https://doi.org/10.1038/s41388-019-1073-2.

[24] Q. Hu, T. Masuda, K. Koike, K. Sato, T. Tobo, S. Kuramitsu, et al., Oxysterol binding protein-like 3 (OSBPL3) is a novel driver gene that promotes tumor growth in part through R-Ras/Akt signaling in gastric cancer, Sci. Rep. 11 (1) (2021) 19178, https://doi.org/10.1038/s41598-021-98485-9.

[25] L. Ponnusamy, S.R. Natarajan, K. Thangaraj, R. Manoharan, Therapeutic aspects of AMPK in breast cancer: progress, challenges, and future directions, Biochimica et biophysica acta Reviews on cancer 1874 (1) (2020) 188379, https://doi.org/10.1016/j.bbcan.2020.188379.

[26] K. Kadono, S. Kageyama, K. Nakamura, H. Hirao, T. Ito, H. Kojima, et al., Myeloid Ikaros-SIRT1 signaling axis regulates hepatic inflammation and pyroptosis in ischemia-stressed mouse and human liver, Journal of hepatology 76 (4) (2022) 896–909, https://doi.org/10.1016/j.jhep.2021.11.026.

[27] S. Zhang, Y. Yang, S. Huang, C. Deng, S. Zhou, J. Yang, et al., SIRT1 inhibits gastric cancer proliferation and metastasis via STAT3/MMP-13 signaling, J. Cell. Physiol. 234 (9) (2019) 15395–15406, https://doi.org/10.1002/jcp.28186.

[28] Z. Zheng, Y. Bian, Y. Zhang, G. Ren, G. Li, Metformin activates AMPK/SIRT1/NF-κB pathway and induces mitochondrial dysfunction to drive caspase3/GSDME-mediated cancer cell pyroptosis 19 (10) (2020) 1089–1104, https://doi.org/10.1080/15384101.2020.1743911.